
RANKL in human periapical granuloma: possible involvement in periapical bone destruction

R Vernal¹, A Dezerega¹, N Dutzan¹, A Chaparro¹, R León², S Chandía³, A Silva⁴, J Gamonal¹

¹Periodontal Biology Laboratory, ²Oral Biology and Biochemistry Laboratory, Dentistry Faculty, University of Chile;

³Immunobiochemistry Laboratory, Chemistry and Pharmacology Sciences Faculty, University of Chile, Santiago, Chile;

⁴Centre for Biological Research, National Center for Scientific Research, Madrid, Spain

OBJECTIVES: The cytokine receptor activator of nuclear factor κ B-ligand (RANKL) has been involved in both the physiological and pathological regulation of osteoclast life span and bone metabolism. Periapical granuloma is a periradicular lesion characterized by periapical bone destruction. The aims of this study were to associate the RANKL mRNA levels to periapical granulomas using the real-time reverse transcriptase-polymerase chain reaction (RT-PCR) technique and to determine the specific cell involved in RANKL synthesis.

METHODS: In eight periapical granuloma and eight periodontal ligament samples from periodontally healthy volunteers, RANKL mRNA was detected by real-time RT-PCR. Expression of RANKL on infiltrate leukocytes was further investigated by flow cytometry in six periapical granulomas.

RESULTS: Receptor activator of nuclear factor κ B-ligand mRNA levels were higher in periapical granulomas than in healthy periodontal ligament as its RANKL mRNA cycle threshold (Ct) and Δ Ct were significantly lower than that of controls (33.07 ± 1.24 vs 36.96 ± 1.69 and 11.58 ± 3.02 vs 15.60 ± 3.31 , respectively). A 16.2-fold (2.0–131.6) higher RANKL gene expression was detected in the granulomas compared with the control tissues. We determined by flow cytometry that lymphocytes were the predominant leukocyte cells (53.31%), and monocytes and dendritic cells were the main RANKL synthesizers in granuloma lesions.

CONCLUSIONS: These data indicate that monocytes synthesized RANKL in periapical granulomas and suggest that RANKL is involved in bone loss associated with periapical lesions.

Keywords: granuloma; immunology; infectious diseases; monocytes; RANKL

Introduction

Periapical lesions are destructive inflammatory pathologies that affect the periapical periodontium. They are characterized by periradicular periodontal ligament and bone destruction as a consequence of bacterial infection of the dental pulp (Wang and Stashenko, 1991; Stashenko *et al*, 1998; Márton and Kiss, 2000). Diverse inflammatory mediators such as interleukin (IL)-1, IL-2, IL-6, IL-8, IL-12, tumor necrosis factor (TNF) $_{\alpha}$, granulocyte-macrophage colony stimulating factor (GM-CSF), nitric oxide (NO), interferon (IFN) $_{\gamma}$, prostaglandins, and metalloproteinases have been associated with periradicular lesions (Stashenko *et al*, 1998; Kawashima and Stashenko, 1999; Shimauchi *et al*, 2001; Ataoglu *et al*, 2002; Shin *et al.*, 2002; Radics *et al*, 2003). In spite of the increasing advance in the knowledge of the pathogenesis of periradicular lesions, the precise bone-resorptive and regulatory cytokines, and the underlying pathologic mechanism associated with periapical bone destruction during its development remain unknown.

Receptor activator of nuclear factor κ B-ligand (RANKL), also known as the osteoprotegerin ligand (OPGL), osteoclast differentiation factor (ODF), TNF-related activation-induced cytokine (TRANCE) and TNF - superfamily member 11 (TNFSF11), has recently been identified as a key regulator of bone metabolism (Lacey *et al*, 1998; Blaque and James, 2003). RANKL is involved in both the physiological and pathological regulation of osteoclastogenesis and osteoclastoactivation (Lacey *et al*, 1998; Takahashi *et al*, 1999; Hofbauer and Heufelder, 2001; Blaque and James, 2003). It has been associated with diverse osteodestructive pathologies, such as rheumatoid arthritis (Kong *et al*, 1999; Theill *et al*, 2002), bone tumors (Huang *et al*, 2000), osteoporosis (Hofbauer and Heufelder, 2001), osteolytic lesions of the facial skeleton (Tay *et al*, 2004), and periodontitis (Teng

et al, 2000; Taubman and Kawai, 2001; Crotti *et al*, 2003; Liu *et al*, 2003; Mogi *et al*, 2004; Vernal *et al*, 2004).

All these data strongly indicate that RANKL is an essential component for osteoclast activation in pathological bone resorption, and thus, could play a role in periapical bone destruction during periapical lesion development. The aims of our study were to determine the RANKL mRNA levels in periapical granuloma samples, a periradicular lesion characterized by periapical bone destruction, using the real-time quantitative reverse transcriptase-polymerase chain reaction (RT-PCR) technique and to investigate the infiltrate leukocyte cells responsible for the local RANKL synthesis, by flow cytometry.

Materials and methods

Patients

The patients for this study were selected from the Postgraduate Center of Diagnostics and Treatment (Faculty of Dentistry, Universidad Complutense, Madrid, Spain). Sixteen patients aged 16–27 years took part in the study. Periapical lesion samples with clinical and radiographic diagnosis of periapical granuloma (PG) were obtained from teeth of eight patients with surgical indication of extraction. As controls, apical periodontal ligament (PL) samples from eight periodontal healthy volunteers were obtained from teeth with orthodontic indication of extraction. For flow cytometry study, five patients, aged 22–25 years, were selected from the Dental Service of Barros Luco Hospital (Southern Metropolitan Health Service, Santiago, Chile). Six PG samples were obtained from teeth with surgical indication of extraction. Subjects did not suffer from systemic illness and had not received antibiotics or non-steroid anti-inflammatory therapy in the 6-month period prior to the study. The protocol was explained to all patients, the Institutional Review Board approved the study and informed consent was obtained from all patients.

Granuloma and PL samples

Both PG lesions and PL tissue were obtained by surgical separation from mineralized tissue of the tooth with curettes (Hu Friedy, Chicago, IL, USA) immediately posterior to teeth extractions. Samples for real-time PCR analysis were submerged in RNAlater (Ambion Inc., Austin, TX, USA) and stored at 4°C for RNA extraction. Samples for flow cytometry analysis were washed extensively in phosphate-buffered saline (PBS) and immediately placed in a vial containing transporting media RPMI1640 supplemented with 50 UI ml⁻¹ penicillin, 50 µg ml⁻¹ streptomycin, and 200 mM L-glutamine (Sigma Chemical Co, St Louis, MO, USA). Vials were transported to the Immunobiochemistry Laboratory (Faculty of Chemistry and Pharmacology Sciences, University of Chile) and processed immediately.

Total RNA extraction

Tissue samples were minced as approximately 1 mm³ fragments and homogenized in 1 ml of TRIzol reagent (Invitrogen Corp., Barcelona, Spain); after incubation for

5 min at room temperature in an RNase-free tube, 0.2 ml of chloroform was added and incubated for 3 min at room temperature. After centrifugation at 12 000 *g* for 15 min at 4°C, the aqueous phase was transferred to a fresh RNase-free tube and RNA was precipitated by mixing it with 0.5 ml of isopropyl alcohol incubated for 10 min at room temperature and centrifuged at 12 000 *g* for 10 min at 4°C. Then, the RNA precipitate was washed once with 1 ml 75% ethanol and centrifuged at 7000 *g* for 5 min at 4°C. Finally, the sample was resuspended in 50 µl of RNase-free water diethylpyrocarbonate (DEPC) 0.1% (Sigma Chemical Co) for 10 min at 60°C. Previous quantification in spectrophotometer, total RNA samples were stored at –80°C in a 250 ng µl⁻¹ concentration until further analysis.

Reverse transcription

First-strand cDNA was synthesized using 500 ng of total RNA with TaqMan[®] Reverse Transcription Reagents (Roche Molecular Systems Inc., Belleville, NJ, USA) according to manufacturer's instruction. Briefly, 30 µl volume reaction containing 3 µl of 10x RT buffer, 6.6 µl of MgCl₂, 6 µl of dNTP mixture, 1.5 µl of Oligo d(T), 0.6 µl of RNase inhibitor, 0.75 µl of Multi Scribe[™] reverse transcriptase, 9.55 µl of RNase-free water and 2 µl of total RNA, were set up in a Primus 96 plus Thermal Cycler (MWG AG Biotech, Ebersberg, Germany) under the following conditions: 10 min at 25°C, 30 min at 48°C and 5 min at 95°C.

Real-time PCR

Real-time quantitative PCR was performed using a specific Assay-on-Demand[™] Gene Expression Products (Applied Biosystems, Foster City, CA, USA), that contained a forward and a reverse primer at non-limiting concentrations and a TaqMan[®] MGB probe 6-FAM[™] dye-labeled, specifically designed to detect and quantify cDNA sequences from multi-exon RANKL gene, without amplifying genomic DNA. Duplicated of 1x and 0.1x dilutions of 83.3 ng cDNA were amplified in a 20 µl volume reaction, that contained 10 µl of TaqMan[®] Universal PCR Master Mix (Applied Biosystems), 1 µl of 20x Assay-on-Demand and 9 µl of cDNA diluted in RNase-free water, under the following conditions: a first step of 2 min at 50°C, a second step of 10 min at 95°C, and 40 cycles of 15 s at 95°C and 1 min at 60°C, in a ABI PRISM[™] 7700 Sequence Detector System (Applied Biosystems). As in the endogenous control assay, 33.3 ng cDNA was amplified to determine the glyceraldehyde-3-phosphate dehydrogenase (GAPDH) mRNA expression, using a TaqMan[®] Pre-Developed Assay Reagent Human GAPDH (Applied Biosystems), in the same dilutions and conditions described for RANKL.

Tissue enzymatic digestion

Periapical granulomas were processed by enzymatic digestion to obtain a total cell suspension (Vernal *et al*, 2005). Briefly, samples were minced into approximately 1 mm³ pieces and incubated in tissue digestion medium at 37°C for 90 min. The tissue digestion medium

consisted of RPMI1640 supplemented with 50 UI ml⁻¹ penicillin, 50 µg ml⁻¹ streptomycin, and 200 mM L-glutamine, plus 200 U ml⁻¹ of type IV collagenase (Gibco Invitrogen Corp., Grand Island, NY, USA). Cells obtained were washed twice with PBS, cell counting was performed in a Neubauer chamber using a phase-contrast microscope (Axiovert 100; Zeiss Co., Göttingen, Germany), and cell viability ≥90% was calculated by Trypan blue dye exclusion. Cells resuspended in PBS were analyzed by flow cytometry.

Flow cytometry analysis of RANKL expression

Fifty microliters of PBS containing 200 000 total cells of each sample was incubated separately with 10 µl of phycoerythrin (PE)- and fluorescein isothiocyanate (FITC)-conjugated anti-CD4 monoclonal antibody (CD4⁺ T cells), anti-CD8 (CD8⁺ T cells), anti-CD14 (monocytes), anti-CD19 (B cells), anti-CD16 and anti-CD56 (natural killer cells), anti-CD62L (neutrophils), and anti-CD84 (dendritic cells) for 30 min at room temperature in the dark (Becton Dickinson Immunocytometry Systems, San José, CA, USA), and with 20 µg ml⁻¹ of mouse anti-human RANKL monoclonal antibody (R&D Systems Inc., Minneapolis, MN, USA) at 4°C overnight, then incubated with 1:64 diluted FITC-conjugated rabbit anti-mouse IgG (R&D Systems Inc.) for 1 h at room temperature. Cells were washed once in PBS and resuspended in 300 µl of PBS to be analyzed by flow cytometry (FACSort, Becton Dickinson Immunocytometry Systems). Cells were gated according their forward- and side-scatter characteristics and their specific CD marker. FITC- and PE-conjugated isotype-matched control monoclonal antibodies were used to determine the positive and negative population. Gates of each specific cell were evaluated for RANKL expression.

Data analysis

Flow cytometry data were analyzed using software WinMDi 2.8 and represented as histograms. RANKL-positive cells were expressed in percentages.

The real-time PCR data were analyzed with the ABI PRISMTM Sequence Detector Systems software version 1.7a (Applied Biosystems). The data were plotted as the ΔRn fluorescence signal vs the cycle number, using the equation: ΔRn = Rn⁺ - Rn⁻, where Rn⁺ is the fluorescence signal of the product at any given time and Rn⁻ is the fluorescence signal of the baseline emission during cycles 3–25 for RANKL and 3–15 for GAPDH. An arbitrary threshold was set by replicate method, where a <0.500 difference was observed between the duplicate data of each sample. The cycle threshold (Ct) value is defined as the cycle number at which the ΔRn crosses this threshold. The relation between RANKL and GAPDH in each individual was defined as ΔCt, where ΔCt = Ct_{RANKL} - Ct_{GAPDH}. The Ct and ΔCt of RANKL and GAPDH of the control and granuloma group were expressed as mean ± standard deviation and data range; the unpaired Student's *t*-test statistic was used to analyze differences. The amplification efficiency between GAPDH and RANKL was

evaluated analyzing the ΔCt variation with template dilutions within a 100-fold range. A plot of ΔCt vs log cDNA dilution was made and the data were fit using least-squares linear regression analysis. The fold change in RANKL relative to the GAPDH endogenous control was determined by the 2^{-ΔΔCt} method (Livak and Schmittgen, 2001).

Results

The clinical characteristics of the patients included in the real-time PCR study are summarized in Table 1. Two males and six females were studied for each group. Mean ages were 21.00 ± 2.62 and 20.38 ± 3.25 years for the granuloma and control group, respectively, and no statistical difference between both groups was found. All PG samples had detectable levels of RANKL (8/8), whereas only 87.5% (7/8) had detectable levels of RANKL in PL samples. The undetectable level is represented by a Ct of 40.000 (Table 1).

Table 2 shows the mean, standard deviation and data range of Ct and ΔCt of RANKL and GAPDH of the granuloma and control group. The GAPDH and RANKL amplification plot of the smaller of each duplicate of granuloma and control group are shown in Figure 1. GAPDH Ct was similar (21.493 ± 2.56 vs 21.360 ± 1.94) but RANKL Ct and the ΔCt was significantly lower in granuloma group than in control group (33.071 ± 1.24 vs 36.959 ± 1.69 and 11.579 ± 3.02 vs 15.599 ± 3.31, *P* = 0.0001 and *P* = 0.02, respectively). The ΔCt variation with 100-fold range dilutions of GAPDH and RANKL (granuloma *n* = 3) shows a slope of 0.0966 (Figure 2); thus, the amplification efficiencies of both amplicons are similar and the fold change in RANKL gene expression

Table 1 Clinical characteristics and Ct RANKL and GAPDH data of periodontal ligament controls and periapical granuloma lesion patients groups

Patients	Gender	Age	RANKL		GAPDH	
			Ct 1	Ct 2	Ct 1	Ct 2
Periodontal ligament						
1	M	24	40.000	40.000	19.080	18.920
2	F	23	38.209	38.018	21.440	21.500
3	F	17	36.676	36.439	22.410	22.340
4	M	18	34.907	34.940	24.320	24.320
5	F	16	36.175	36.311	19.090	18.880
6	F	24	34.936	35.198	22.030	22.020
7	F	22	38.030	37.959	19.800	19.750
8	F	19	36.834	36.710	22.710	23.150
Periapical granuloma						
1	F	21	33.721	33.775	17.180	17.230
2	F	20	34.706	34.671	20.350	20.220
3	F	27	33.268	32.779	19.590	19.600
4	F	20	30.875	31.114	22.740	22.720
5	F	19	33.073	33.321	21.060	20.950
6	F	22	31.455	31.652	21.960	21.620
7	M	20	33.203	33.291	24.290	24.220
8	M	19	34.131	34.101	25.020	25.130

Gender (M, male, F, female), age (years); Ct, threshold cycle (duplicates).

Table 2 Ct of RANKL and GAPDH, and Δ Ct between RANKL and GAPDH from granuloma and control groups

	Granuloma group (n = 8)	Control group (n = 8)
Ct _{GAPDH}		
mean \pm s.d.	21.493 \pm 2.56	21.360 \pm 1.94
range	17.205–25.075	18.985–24.320
Ct _{RANKL}		
mean \pm s.d.	33.071 \pm 1.24*	36.959 \pm 1.69
range	30.995–34.689	34.924–40.000
Δ Ct		
mean \pm s.d.	11.579 \pm 3.02**	15.599 \pm 3.31
range	8.265–19.543	10.604–21.000
$2^{-\Delta\Delta Ct}$		
Fold	16.2 (2.0–131.6)	1.0 (0.1–9.9)

Fold change of RANKL from granuloma vs control group using $2^{-\Delta\Delta Ct}$ method (fold change and estimated error).

*Granuloma vs control groups, $P = 0.0001$.

**Granuloma vs control groups, $P = 0.02$.

may be represented by the $2^{-\Delta\Delta Ct}$ method. The relative quantification of RANKL was determined using the $2^{-\Delta\Delta Ct}$ method, in PG samples there was a 16.2-fold increase in the RANKL expression compared with PL samples, with an exponential range of estimated error of 2.0–131.6 (Table 2).

Figure 3 features side- and forward-scatter density plot and histograms of CD marker and RANKL expression of dendritic cells (CD83⁺) and monocytes

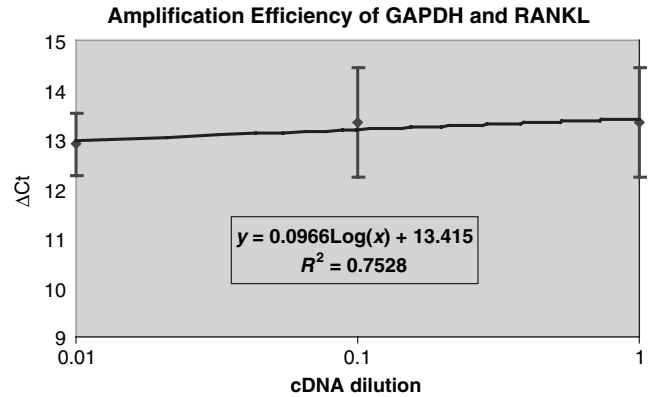


Figure 2 Efficiency of RANKL and GAPDH amplification by real-time PCR. Serial dilutions of cDNA (1 to 0.01) were amplified by real-time PCR using gene-specific primers and were detected by TaqMan[®] probes. The Δ Ct (Ct_{RANKL} – Ct_{GAPDH}) average and standard deviation of $n = 3$ granuloma samples were calculated for each volume of cDNA that was amplified. A plot of the log cDNA dilution vs Δ Ct was made and the data were fit using least-squares linear regression analysis. The slope was 0.0966, thus, the amplification efficiencies of both amplicons are similar and the fold change in RANKL gene expression may be represented by $2^{-\Delta\Delta Ct}$ method

(CD14⁺). The cells were gated and the results of monoparametric analyses of gated cells with the different antibodies are shown. The complete results of flow cytometry analysis are summarized in Table 3; 53.31%

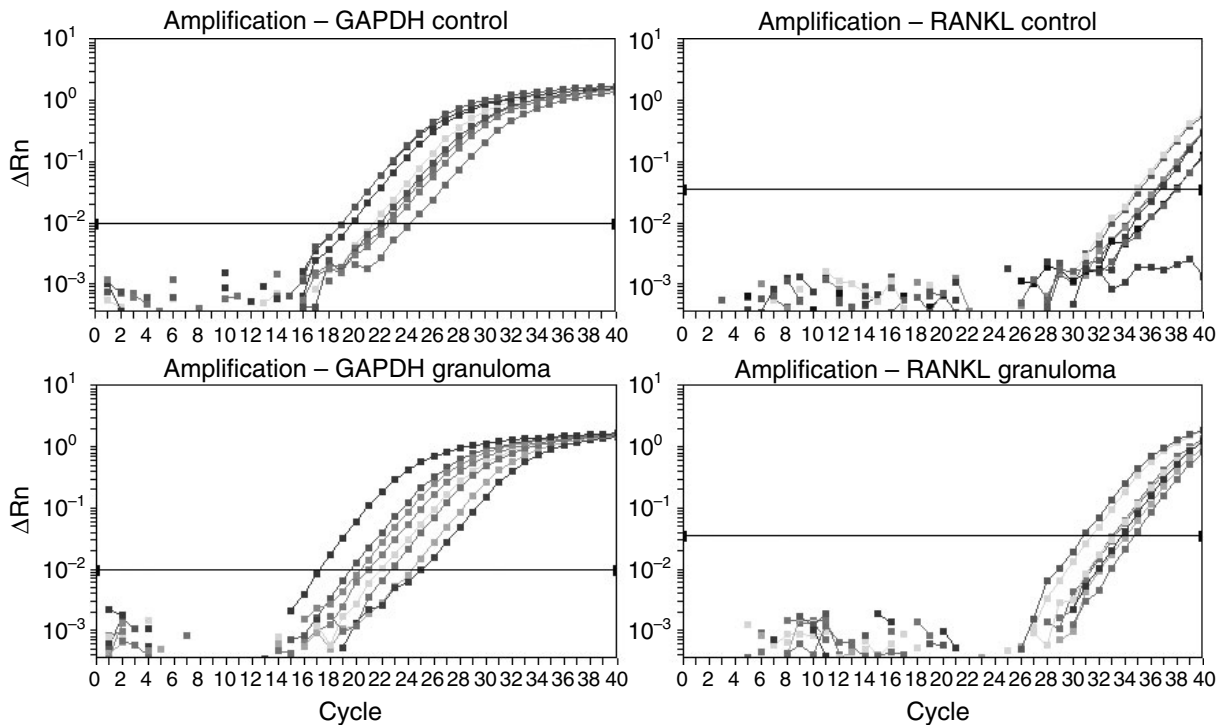


Figure 1 GAPDH and RANKL amplification plot for periodontal ligament control and granuloma groups. The real-time PCR of the smaller data of the each duplicate were plotted as the Δ Rn fluorescence signal vs the cycle number, using the equation $\Delta Rn = Rn^+ - Rn^-$; Rn^+ is the fluorescence signal of the product at any given time and Rn^- the fluorescence signal of the baseline during cycles 3–25 for RANKL and 3–15 for GAPDH. An arbitrary threshold was set using the replicate method. The Ct value was defined as the cycle number at which the Δ Rn crosses this threshold

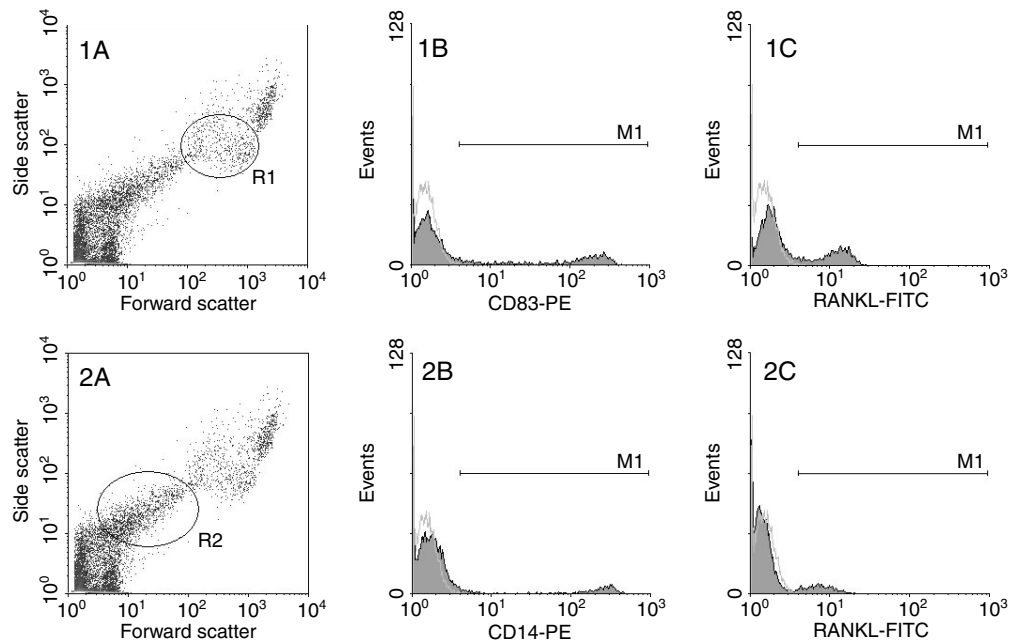


Figure 3 Immunotypification by flow cytometry of dendritic cells and monocytes obtained by enzymatic tissue digestion of six periapical granulomas. (1A) Side- and forward-scatter density plot of gated dendritic cells; (1B) histogram of CD83⁺ cells; (1C) histogram of RANKL⁺ dendritic cells; (2A) side- and forward-scatter density plot of gated monocytes; (2B) histogram of CD14⁺ cells; (2C) histogram of RANKL⁺ monocytes

Table 3 Marker and RANKL on immune cells from periapical granulomas analysed by flow cytometry

Cell type	Marker	Percentage
Lymphocytes T CD4	CD4	5.81
Lymphocytes T CD8	CD8	21.02
Lymphocytes B	CD19	11.57
Natural killer cytotoxic cells	CD16	6.49
Natural killer secretory cells	CD56	8.42
Monocytes	CD14	13.33
Dendritic cells	CD83	18.62
Neutrophils	CD62L	2.75
RANKL	RANKL	26.66
RANKL ⁺ monocytes	RANKL	13.11
RANKL ⁺ dendritic cells	RANKL	13.55

CD, Clusters of differentiation.

of the analyzed cells were lymphocytes. Among lymphocytes, 26.83% were T cells, 11.57% were B cells (CD19) and 14.91% were natural killer cells. Among T lymphocytes, 5.81% and 21.02% were CD4 and CD8 cells, respectively. Among natural killer cells, 6.49% were cytotoxic (CD16) and 8.42% were secretory cells (CD56). Monocytes (CD14) were 13.33%, neutrophils (CD62L) were 2.75% and dendritic cells (CD83) were 18.62% of the isolated cells; 26.66% of the total isolated cells expressed RANKL; 13.11% of this expression was associated with monocytes and 13.55 with dendritic cells.

Discussion

We have examined the RANKL mRNA levels in periapical granuloma lesions. Using specific probes for

RANKL and a real-time quantitative RT-PCR technique, we have demonstrated that the levels of RANKL mRNA were significantly higher in PG than in healthy PL control samples.

The periapical lesion represents an inflammatory and immune response against microorganisms that invade and destroy the dental pulp (Wang and Stashenko, 1991; Stashenko *et al*, 1998; Márton and Kiss, 2000). The pathologic response appears to be similar to that which occurs in response to bacterial infections elsewhere in the body, with the additional feature that alveolar bone surrounding the root apex is resorbed (Kawashima and Stashenko, 1999).

Using small tissue biopsies it is possible to analyze the levels of specific cytokines being produced during the inflammatory process associated with tissue destruction and optimizes the measure of its transcriptional activity. Using quantitative RT-PCR with specific primers and TaqMan[®] probes for RANKL, we have determined that the Ct and Δ Ct of RANKL in PG samples were lower than those observed in PL samples. Because of the fact that Ct values decrease linearly with increasing input target quantity (Giulietti *et al*, 2001), RANKL mRNA levels were higher in granuloma group than in the control group. This finding is in correspondence with our previous studies in periodontal disease, where we clearly demonstrated a relationship between RANKL and the marginal alveolar bone destruction observed in chronic periodontitis (Vernal *et al*, 2004).

Periodontitis and periapical lesions are characterized by alveolar bone destruction as a consequence of bacterial infection, and in both pathologies it has been proposed that inflammatory bone resorption may be upregulated *in vivo* by T-helper (Th)1-type mediators

and downregulated by Th2-type mediators (Kawashima and Stashenko, 1999).

The periradicular cellular infiltrate in periapical lesions is mainly characterized by macrophages, and T and B cells (Matsuo *et al*, 1992). CD4⁺ T cells are the predominant lymphocyte cells (Sol *et al*, 1998) and they have been shown to be the principal cells observed in the acute state of pathologic development (Leonardi *et al*, 2000).

In other bone-destructive diseases, it has been shown that activated CD4⁺ T cells participate directly in pathologic bone destruction through RANKL expression (Kong *et al*, 1999; Taubman and Kawai, 2001; Theill *et al*, 2002).

We characterized the cells subpopulations in six periapical PGs by flow cytometry. In agreement with a previous flow cytometry study (Sol *et al*, 1998) the predominant isolated cells in our work were lymphocytes. Unlike them, we observed monocytes after the enzymatic digestion phase performed before the flow cytometric analysis. Monocytes–macrophages have been established as important constituents of PGs and macrophage activity has been associated with the development of periapical lesions and bone destruction through secretion of bone-resorbing cytokines (Metzger, 2000). The presence of macrophages in human periapical inflammatory lesions has been a commonly reported finding (Stern *et al*, 1982; Piattelli *et al*, 1991). Macrophages may also serve as antigen-presenting cells as the dendritic cells. In our study, both of them were isolated in high levels. They process the antigen and present it to the antigen-specific clones of CD4⁺ T cells by a process involving major histocompatibility complex (MHC) II molecules. On the contrary, macrophages are considered a main source of cytokines (IL-1 α , IL-1 β and TNF α), matrix metalloproteinases (MMPs) and prostaglandins, that contribute to the inflammatory process and to the destructive outcome of the periapical lesions (Metzger, 2000). Our results clearly associate the higher RANKL levels observed in the PG lesions to the monocyte activity, thus, activated macrophage would participate in the formation as well as the perpetuation of the periapical lesions.

Receptor activator of nuclear factor κ B-ligand is an important regulator of the interactions between T cells and dendritic cells during the antigen presentation process. RANKL is also expressed on the surface of the dendritic cells and the interaction with its receptor can induce cluster formation and activation of T cells, dendritic cell survival, regulate the dendritic cell functions, and T cell–dendritic cell communication (Theill *et al*, 2002).

Receptor activator of nuclear factor κ B-ligand is a bone-resorptive cytokine that has been established as an essential molecule in all phases of the osteoclast's life span, and it has been catalogued as a key regulator of the physiological and pathological control of bone metabolism (Lacey *et al*, 1998; Takahashi *et al*, 1999; Hofbauer and Heufelder, 2001; Blaque and James, 2003). RANKL has been associated with diverse pathologies characterized by bone destruction, such as rheumatoid arthritis, osteoporosis, Paget's disease, bone

tumors, facial osteolytic lesions and periodontitis (Kong *et al*, 1999; Huang *et al*, 2000; Teng *et al*, 2000; Hofbauer and Heufelder, 2001; Taubman and Kawai, 2001; Theill *et al*, 2002; Crotti *et al*, 2003; Liu *et al*, 2003; Mogi *et al*, 2004; Tay *et al*, 2004; Vernal *et al*, 2004). It has been proposed as the common final pathway of the bone-resorptive and regulatory cytokines, in osteoclast differentiation and activation and in bone resorption.

A complex network of cytokines is secreted in the periapex in response to the pulp infection by fibroblasts and infiltrates macrophage–monocytes and lymphocytes (Kawashima *et al*, 1996). This cytokine network stimulates osteoclast activity and the periapical bone resorption through a not yet completely known mechanism. The RANKL participation in the periradicular bone destruction is an interesting proposed pathway through which it is possible to explain the participation of the diverse cytokines associated to its pathogenesis.

Using the 2^{- $\Delta\Delta$ Ct} method (Livak and Schmittgen, 2001), our data show that in PG samples the RANKL expression was increased 16.2-fold in comparison with the control group, with an exponential range of estimated error of 2.0–131.6, indicating that RANKL gene is highly over-expressed in granuloma lesions associated with periapical bone destruction.

These results demonstrate a clear relation between high RANKL levels and monocyte activity during periapical bone destruction in periapical granuloma. Given the central role of RANKL in the pathogenesis of other bone-destructive diseases, our findings indicate that RANKL plays a key role in the pathologic events associated with periradicular bone destruction, and that methods for controlling RANKL activity would be reasonable as a means of treating these disorders.

Acknowledgements

This research was supported by grant 1050518 of Fondo de Investigación Científica y Tecnológica (FONDECYT), grant 01/0073-01 of Fondo de Investigaciones Sanitarias (FIS), and grant PG/2503 of Vicerrectoría Académica y Departamento de Posgrado y Postítulo of Universidad de Chile. The authors are grateful to Dr Raúl Sáez from Dental Service of Barros Luco Hospital.

References

- Ataoglu T, Üngör M, Serpek B, Haliloglu S, Ataoglu H, Ari H (2002). Interleukin-1 β and tumor necrosis factor- α levels in periapical exudates. *Int Endod J* **35**: 181–185.
- Blaque S, James I (2003). RANKL (receptor activator of NF κ B ligand). In: Thomson AW, Lotze MT, eds. *The Cytokine Handbook*. Academic Press: London, pp. 871–883.
- Crotti T, Smith MD, Hirsch R *et al* (2003). Receptor activator NF κ B ligand (RANKL) and osteoprotegerin (OPG) protein expression in periodontitis. *J Periodont Res* **38**: 380–387.
- Giulietti A, Overbergh L, Valckx D, Decallonne B, Bouillon R, Mathieu Ch (2001). An overview of real-time quantitative PCR: applications to quantify cytokine gene expression. *Methods* **25**: 386–401.

- Hofbauer LC, Heufelder AE (2001). Role of receptor activator of nuclear factor- κ B ligand and osteoprotegerin in bone cell biology. *J Mol Med* **79**: 243–253.
- Huang L, Xu J, Wood DJ, Zheng MH (2000). Gene expression of osteoprotegerin ligand, osteoprotegerin, and receptor activator of NF- κ B in giant cell tumor of bone. Possible involvement in tumor cell-induced osteoclast-like cell formation. *Am J Pathol* **156**: 761–767.
- Kawashima N, Stashenko P (1999). Expression of bone-resorptive and regulatory cytokines in murine periapical inflammation. *Arch Oral Biol* **44**: 55–66.
- Kawashima N, Okiji T, Kosaka T, Suda H (1996). Kinetics of macrophages and lymphoid cells during the development of experimentally induced periapical lesions in rat molars: a quantitative immunohistochemical study. *J Endod* **22**: 311–316.
- Kong YY, Feige U, Sarosi I *et al* (1999). Activated T cells regulate bone loss and joint destruction in adjuvant arthritis through osteoprotegerin ligand. *Nature* **402**: 304–309.
- Lacey DL, Timms E, Tan HL *et al* (1998). Osteoprotegerin ligand is a cytokine that regulates osteoclast differentiation and activation. *Cell* **93**: 165–176.
- Leonardi R, Lanteri E, Stivala F, Travali S (2000). Immunolocalization of CD44 adhesion molecules in human periradicular lesions. *Oral Surg Oral Med Oral Pathol Oral Radiol Endod* **89**: 480–485.
- Liu D, Xu JK, Figliomeni L *et al* (2003). Expression of RANKL and OPG mRNA in periodontal disease: possible involvement in bone destruction. *Int J Molec Med* **11**: 17–21.
- Livak KJ, Schmittgen TD (2001). Analysis of relative gene expression data using real-time quantitative PCR and the $2^{-\Delta\Delta C_t}$ method. *Methods* **25**: 402–408.
- Márton IJ and Kiss C (2000). Protective and destructive immune reactions in apical periodontitis. *Oral Microbiol Immunol* **15**: 139–150.
- Matsuo T, Ebisu S, Shimabukuro Y, Ohtake T, Okada H (1992). Quantitative analysis of immunocompetent cells in human periapical lesions: correlations with clinical findings of the involved teeth. *J Endod* **18**: 497–500.
- Metzger Z (2000). Macrophages in periapical lesions. *Endod Dent Traumatol* **16**: 1–8.
- Mogi M, Otogoto J, Ota N, Togari A (2004). Differential expression of RANKL and osteoprotegerin in gingival crevicular fluid of patients with periodontitis. *J Dent Res* **83**: 166–169.
- Piattelli A, Artese L, Rosini S, Quantara M, Musiani P (1991). Immune cells in periapical granuloma: morphological and immunohistochemical characterization. *J Endod* **17**: 26–29.
- Radics T, Kiss C, Tar I, Márton IJ (2003). Interleukin-6 and granulocyte-macrophage colony-stimulating factor in apical periodontitis: correlation with clinical and histologic findings of the involved teeth. *Oral Microbiol and Immunol* **18**: 9–13.
- Shimauchi H, Takayama S, Narikawa-Kiji M, Shimabukuro Y, Okada H (2001). Production of interleukin-8 and nitric oxide in human periapical lesions. *J Endod* **27**: 749–752.
- Shin SJ, Lee JI, Baek SH, Lim SS (2002). Tissue levels of matrix metalloproteinases in pulps and periapical lesions. *J Endod* **28**: 313–315.
- Sol MA, Tkaczuk J, Voight JJ *et al* (1998). Characterization of lymphocyte subpopulations in periapical lesions by flow cytometry. *Oral Microbiol Immunol* **13**: 253–258.
- Stashenko P, Teles R, D'Souza R (1998). Periapical inflammatory responses and their modulation. *Crit Rev Oral Biol Med* **9**: 498–521.
- Stern MH, Dreizen S, Mackler BF, Levy BM (1982). Isolation and characterization of inflammatory cells from the human periapical granuloma. *J Dent Res* **61**: 1408–1412.
- Takahashi N, Udagawa N, Suda T (1999). A new member of Tumor Necrosis Factor Ligand Family, ODF/OPGL/TRANCE/RANKL, regulates osteoclast differentiation and function. *Biochem Biophys Res Commun* **256**: 449–455.
- Taubman MA, Kawai T (2001). Involvement of T-lymphocytes in periodontal disease and in direct and indirect induction of bone resorption. *Crit Rev Oral Biol Med* **12**: 125–135.
- Tay JY, Bay BH, Yeo JF, Harris M, Meghji S, Dheen ST (2004). Identification of RANKL in osteolytic lesions of the facial skeleton. *J Dent Res* **83**: 349–353.
- Teng YT, Nguyen H, Gao X *et al* (2000). Functional human T-cell immunity and osteoprotegerin ligand control alveolar bone destruction in periodontal infection. *J Clin Invest* **106**: 59–67.
- Theill LE, Boyle WJ, Peninger JM (2002). RANK-L and RANK: T cells, bone loss, and mammalian evolution. *Annu Rev Immunol* **20**: 795–823.
- Vernal R, Chaparro A, Graumann R, Puente J, Valenzuela MA, Gamonal J (2004). Levels of Cytokine Receptor Activator of Nuclear Factor κ B Ligand in Gingival Crevicular Fluid in Untreated Chronic Periodontitis Patients. *J Periodontol* **75**: 1586–1591.
- Vernal R, Dutzan N, Chaparro A, Puente J, Valenzuela MA, Gamonal J (2005). Levels of interleukin-17 in gingival crevicular fluid and in supernatants of cellular cultures of gingival tissue from patients with chronic periodontitis. *J Clin Periodontol* **32**: 383–389.
- Wang C and Stashenko P (1991). Kinetics of bone-resorbing activity in developing periapical lesions. *J Dent Res* **70**: 1362–1366.
-